



Green tea ameliorates the side effects of the silver nanoparticles treatment of Ehrlich ascites tumor in mice

Ahmed Magdy¹ · Emad Sadaka¹ · Nemanly Hanafy² · Mohammed A. El-Magd³ · Nasr Allahloubi⁴ · Maged El Kemary²

Accepted: 19 March 2020 / Published online: 31 March 2020
© The Korean Society of Toxicogenomics and Toxicoproteomics 2020 2020

Abstract

Background Silver nanoparticles (AgNPs) have anti-cancer effects with fewer side effects than standard chemotherapeutic agents, however, they exert oxidative stress-based adverse effects on normal cells and so their applications have raised concern about possible health and environmental risks.

Objective We evaluated whether green tea extract (GTE), which contains potent antioxidants, could ameliorate AgNPs geno-, cyto-, and histotoxicities without decreasing their therapeutic potential against Ehrlich ascetic carcinoma (EAC).

Results GTE enhanced the anti-cancer effect of AgNPs against EAC cells and ameliorated the genotoxic effect of AgNPs as indicated by lowering chromosomal aberrations and micronucleus frequencies. Additionally, GTE relieved most of degenerative histological changes induced by AgNPs. GTE restored the increased MDA and the decreased SOD, GPx and CAT serum levels induced by AgNPs to levels comparable to normal. The pre-treatment with GTE and AgNPs showed better improvement than the post-treatment strategy.

Conclusions GTE can not only ameliorate AgNPs-induced adverse effects but also improve their anti-cancer effect against EAC. So, it could be useful in the treatment of liver dysfunction associated with AgNPs.

Keywords Silver nanoparticles · Ehrlich ascetic carcinoma · Green tea extract · Oxidative stress · Genotoxicity · Hepatotoxicity

Introduction

While medical technology has improved, cancer remains a serious health problem and has been recognized as an important factor in mortality and morbidity. Cancer is the second leading cause of death worldwide. Cancer chemotherapies have nonspecific toxicity due to their biodistribution

throughout the body which requires administration of a large dose to achieve high local concentrations in tumor (El-Magd et al. 2017; Khamis et al. 2018). Most chemotherapeutic agents also induce formation of multidrug resistance in patients which interferes with their therapeutic potential (Gottesman et al. 2002). Therefore, it is necessary to develop bioessential and non-toxic anti-cancer agents as new alternative plans for overcoming constraints during current chemotherapy (Badawy et al. 2019; Elgazar et al. 2018; Elkeiy et al. 2018).

Because of its anti-bacterial properties, silver nanoparticles (AgNPs) have been widely used in a wide range of medical care and consumer products (Jia et al. 2017). Previous studies denoted that AgNPs had anti-cancer effects against a large variety of cancers (such as ovarian, breast and cervical cancers) and inhibitory effects against microorganisms (such as fungi and bacteria) and these cytotoxic effects are mainly mediated through induction of apoptosis-dependent oxidative stress (Anandalakshmi et al. 2016; Devaraj et al. 2013; Gurunathan et al. 2015; Lee et al. 2019; Lin et al.

✉ Ahmed Magdy
Ahmed_magdy@med.kfs.edu.eg

✉ Mohammed A. El-Magd
mohamed.abouelmagd@vet.kfs.edu.eg

¹ Clinical Oncology and Nuclear Medicine, Faculty of Medicine, Kafrelsheikh University, Kafr El-Shaikh, Egypt

² Institute of Nanoscience and Nanotechnology, Kafrelsheikh University, Kafr El-Shaikh, Egypt

³ Department of Anatomy, Faculty of Veterinary Medicine, Kafrelsheikh University, Kafr El-Shaikh, Egypt

⁴ Department of Medical Oncology, National Cancer Institute, Cairo University, Cairo, Egypt

2014). Increased production and utilization of AgNPs-based products ultimately increased the accumulation of AgNPs in environment and human tissues. Although AgNPs have anti-cancer effects with less toxicity than chemotherapeutic agents, they still have some adverse effects on normal cells. AgNPs can penetrate cell membrane and bind to DNA and protein causing apoptosis not only for cancer cells but also for normal cells (Ahamed et al. 2008; Cho et al. 2018; Jeyaraj et al. 2013). Rats injected with AgNPs showed testicular degenerative changes accompanied by increased levels of oxidative markers and decreased levels of antioxidant markers (Ansar et al. 2017). Additionally, mice intraperitoneally injected with AgNPs at different sizes (10, 60, and 100 nm) showed histopathological changes in their hepatic tissues (congestion, vacuolation, necrosis, and apoptosis) only with smaller AgNPs (10 nm) (Cho et al. 2018). Similarly, no degenerative changes were observed in the majority of mice organs (liver, kidney, brain, lung, testis, spleen) following injection of larger AgNPs (100 nm) (Kanipandian et al. 2019). However, little is known regarding geno-, cyto-, and histotoxicities induced by small AgNPs during treatment of Ehrlich ascetic carcinoma (EAC) in mice.

Dietary natural products were reported to have many biologic activities including antioxidant and anti-cancer properties (Abu Gazia and El-Magd, 2018a; Abu Khudir et al. 2019; Badawy et al. 2019; El-Magd et al. 2019; Elkeiy et al. 2018; Khamis et al. 2018; Mohamed et al. 2019). Hence, researchers search for natural products with anti-cancer effect which can be individually or synergistically used with anti-cancer agents (chemotherapeutic and NPs) to improve therapeutic potential and decrease side effects. Green tea is a popular and globally consumed beverage and its active components (potent antioxidant polyphenolic flavonoids, including catechins gallate and epigallocatechin) are found in various herbal and dietary supplements (Chacko et al. 2010). Green tea extract (GTE) has anticarcinogenic, antiviral, anti-inflammatory, and antidiabetic activities (Abdel-Daim et al. 2017; Miyata et al. 2018). Moreover, green tea catechins alone prevent prostate cancer development in patients with high-grade intraepithelial neoplasia (Bettuzzi et al. 2006) and when used in combination with anti-cancer drugs synergistically induce apoptosis in human cancer cells and inhibit tumor formation in mice (Fujiki et al. 2002). However, to best of our knowledge, the combined anti-cancer effect of AgNPs and GTE on EAC is still unknown. Therefore, we hypothesized that GTE could ameliorate AgNPs oxidative stress-based adverse effects without decreasing their therapeutic potential against EAC in mice. This study was performed to assess this hypothesis.

Materials and methods

Preparation and characterization of silver nanoparticles

Silver nanoparticles (AgNPs) were prepared by chemical reduction method. In brief, 1000 ml of 0.001 M silver nitrate (AgNO₃, purity 99.9%, Sigma-Aldrich) was heated, then 20 ml of 2% trisodium citrate (purity 99%, Sigma-Aldrich) was added dropwise, followed by vigorous mixing until the color change was evident (pale yellow). AgNPs pellet was then separated by centrifugation at 9000 rpm for 30 min and was suspended in double distilled water to obtain the desired concentration. The characterization of AgNPs was performed by Fourier transform infrared (FTIR) spectroscopy, X-ray diffraction, and UV–Vis spectroscopy as previously described (Anandalakshmi et al. 2016; Devaraj et al. 2013).

Preparation of green tea aqueous extract

The aqueous extraction of green tea was prepared as previously described (Safer et al. 2012). Briefly, dried Japanese tea leaves (500 g) purchased from a local store were powdered in a waring blender and extracted with double distilled water (2 L) at 80 °C for 1 h. The extract was filtered through a nylon filter and the filtrate was centrifuged at 3000×g for 15 min. The clear supernatant was removed and the residual pellet was shaken with distilled water, warmed at 35 °C, and centrifuged again. The supernatants were pooled and lyophilized under freezing and the resulting material was stored at –20 °C in a screw-capped bottle.

Animals and experimental design

All experiments were conducted in accordance with US National Institutes of Health Guidelines for the Care and Use of Laboratory Animals and followed Helsinki declaration of animal ethics. This study was approved by the Research Ethics Committee of Kafrelsheikh University.

A total number of sixty adult male Swiss albino mice with weight ranging from 25 to 32 g were used in the present study. These mice were housed in metal cages and received food (basal diet) ad libitum. They also had free access to water. They were raised under a light/dark system of 12 h/12 h. The animals were accommodated to the laboratory conditions for 1 week before the experiment.

The mice were divided into six groups. In group 1 (G1, normal), mice were intraperitoneally (i.p.) injected with 0.2 ml saline daily for 16 days. In G2 (EAC), mice were i.p. inoculated with a single dose of 0.2 ml EAC cells with a total count of 2.5×10^6 and kept for 8 days until the abdomen

reached maximal distention. In G3 (AgNPs pre-treatment), mice were i.p. injected with 10–50 nm AgNPs at a dose of 0.3 mg/kg body weight (bw) daily for 8 days (Cho et al. 2018) and then were i.p. inoculated at the 9th day with EAC cells once and kept for additional 8 days (from the 9th to 16th day of the experiment). In G4 (AgNPs + GTE pre-treatment), mice were injected with AgNPs (as stated in G3) and were orally given GTE at a concentration of 200 mg/Kg bw with a volume of 0.5 ml per mouse (Safer et al. 2012) daily for 8 days and then were i.p. inoculated with EAC cells (as detailed in G3). In G5 (AgNPs post-treatment), mice were i.p. inoculated with EAC cells once and kept for 8 days and then were injected with AgNPs at the 9th day and continued till the 16th day. In G6 (AgNPs + GTE post-treatment), mice were i.p. inoculated with EAC cells once and kept for 8 days and then were treated with AgNPs and GTE from the 9th to the 16th day.

At the end of the experiment, the peritoneal fluids containing EAC cells were collected by a clean syringe, blood samples were collected in clean tubes either with (for micronucleus assay) or without EDTA for serum separation (for biochemical assays) (Badawy et al. 2018). Animals were euthanized by decapitation and livers (for histopathology) and femurs (for chromosomal aberrations) were obtained.

Cell count and viability

Trypan blue exclusion test was performed as previously described (El-Magd et al. 2017). In this test, EAC cells were counted via hemocytometer after staining with 0.5% trypan blue: the percentage of viable cells = [(total number of cells – number of trypan blue (dead) cells)/total number of cells] × 100.

Micronucleus and chromosomal aberrations assays

Blood smears were air dried for 24 h, fixed in ethyl alcohol for 10 min, and stained by 10% Giemsa staining for 10 min. Three slides were prepared from each mouse and 1000 erythrocytes of each mouse were examined under oil immersion at × 1000 for presence of micronuclei (Fenech et al. 2003). Chromosomes of bone marrow somatic cells were prepared and examined as previously described (Pacchierotti and Stocchi 2013).

Histopathological investigation

For light microscope examination, liver specimens were fixed in 10% formalin, dehydrated in ethyl alcohol, cleaned in xylene, embedded in paraffin, cut into 5 µm sections, and stained by hematoxylin and eosin (H & E). For transmission electron microscope (TEM), liver specimens were fixed in 2.5% glutaraldehyde and 1% osmium tetroxide. The sections

were dehydrated in ascending grades of ethanol ending with propylene oxide and embedded in epoxy resin. Ultrathin sections were cut on an RMC MT6000-XL ultramicrotome, mounted on copper grids, stained with uranyl acetate and lead citrate, and examined using TEM-100 CXII operating at 80 kV (Abu Gazia and El-Magd, 2018b).

Biochemical analysis

The level of lipid peroxidation biomarker malondialdehyde (MDA) and activities of antioxidant enzymes [catalase (CAT), glutathione peroxidase (GPx), and superoxide dismutase (SOD)] were determined in serum using commercially available kits (Biodiagnostic, Egypt) and as previously described (El-Bayomi et al. 2018).

Statistical analysis

The results were expressed as mean ± standard error of mean (SEM). Data were statistically analyzed by GraphPad Prism Software 7 (LaJolla, CA, USA) using one-way analysis of variance (ANOVA) followed by Duncan's test for comparison between different treatment groups. Statistical significance was set at $P \leq 0.05$.

Results

Characterization of silver nanoparticles

The physicochemical properties of nanoparticles are important for their behavior, biodistribution, safety, and efficacy. Figure 1 shows characterization of prepared AgNPs using Fourier transform infrared (FTIR) spectroscopy, X-ray diffraction (XRD), and UV–Vis spectroscopy. The latter showed an absorption peak at 411 nm indicating the formation of AgNPs (Devaraj et al. 2013). XRD pattern of AgNPs showed main diffraction peaks at $2\theta = 37^\circ$, 44° , 64° and 76° that were attributed to (111), (200), (220) and (311) planes, respectively (Anandalakshmi et al. 2016). FTIR of AgNPs also showed two prominent peaks at 3449 assigned to stretching vibrations of O–H groups. While, there was a strong absorption band at 1637/cm that was assigned to the C=O stretching vibration in carboxylic group and NH bending vibration of amines (Marimuthu et al. 2011). The TEM image of the prepared AgNPs revealed that the particles ranged in size from 10 to 50 nm, with an average size of ~29 nm.

GTE improved the anti-cancer effect of AgNPs on EAC cells

Previous studies reported anti-cancer effect for AgNPs and GTE each alone but not in combination. To evaluate their

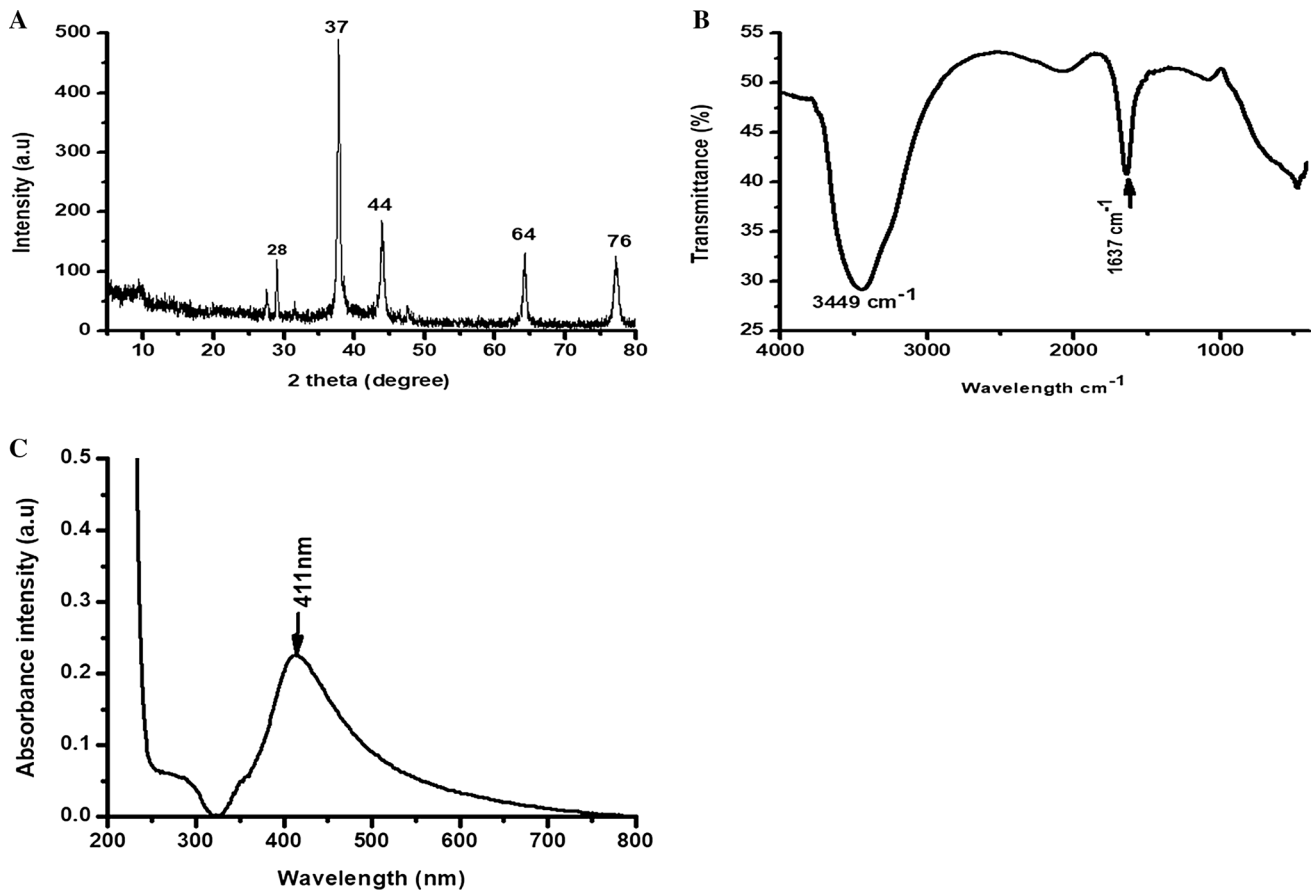


Fig. 1 Characterization of prepared AgNPs. **a** XRD of AgNPs with the main peaks at (2θ) 37, 44, 64 and 76 corresponding to the (111), (200), (220) and (311) planes, respectively. **b** FTIR spectra of AgNPs

exhibited prominent peaks at 3449 and 1637 cm^{-1} . **c** UV-Vis absorption spectrum of AgNPs with silver surface plasmon resonance band occurring initially at 411 nm

combinatory effect on EAC cells, we determined changes in EAC cell counts (total, dead and viable) and tumor volume. The obtained results revealed that EAC mice either pre (G4)- or post (G6)-treated with AgNPs and GTE in combination gave better anti-cancer effect (as evidenced by a significant reduction in total and viable EAC cells, tumor volume and a significant increase in dead tumor cells) than untreated EAC mice (G2) and EAC pre (G3)- or post (G5)-treated with AgNPs alone (Fig. 2). Moreover, pre-treatment strategy resulted in better anti-cancer effect than post-treatment strategy.

GTE ameliorated the genotoxic effect of AgNPs

The genotoxic effect of AgNPs was evaluated using peripheral blood micronucleus test and the obtained results (Fig. 3) exhibited a significant increase in erythrocyte micronucleus frequencies in untreated EAC mice (G2), AgNPs pre (G3)- and post (G5)- treated EAC mice as compared to the control group (G1). Again, combined pre (G4)- and post (G6)-treatment of GTE and AgNPs showed significant decrease in

micronucleus frequencies, with lowest level in G4, relative to other treated groups (G3 and G5).

To confirm GTE ameliorative effect on AgNPs genotoxicity, we evaluated the combined effects of AgNPs and GTE on bone marrow somatic cells chromosomal distribution. The obtained data (Table 1 and Fig. 4) revealed the presence of a significantly higher number of several chromosomal aberrations (ring, deletion, centromeric attenuation and end-to-end association) in untreated EAC mice (G2) and EAC mice treated with AgNPs (G3 and G5) than in the control group (G1). This elevated number of aberrations was significantly decreased following combined treatment with GTE. Again, chromosomal aberration showed significant decrease in pre-treated groups relative to post-treated groups.

Effect of AgNPs and GTE on liver histology

Light microscope examination of stained liver tissues of mice in the control group (G1) revealed presence of normal hepatic architecture in form of normal hepatic parenchyma with preserved hepatic cords (arrows) radiating from the

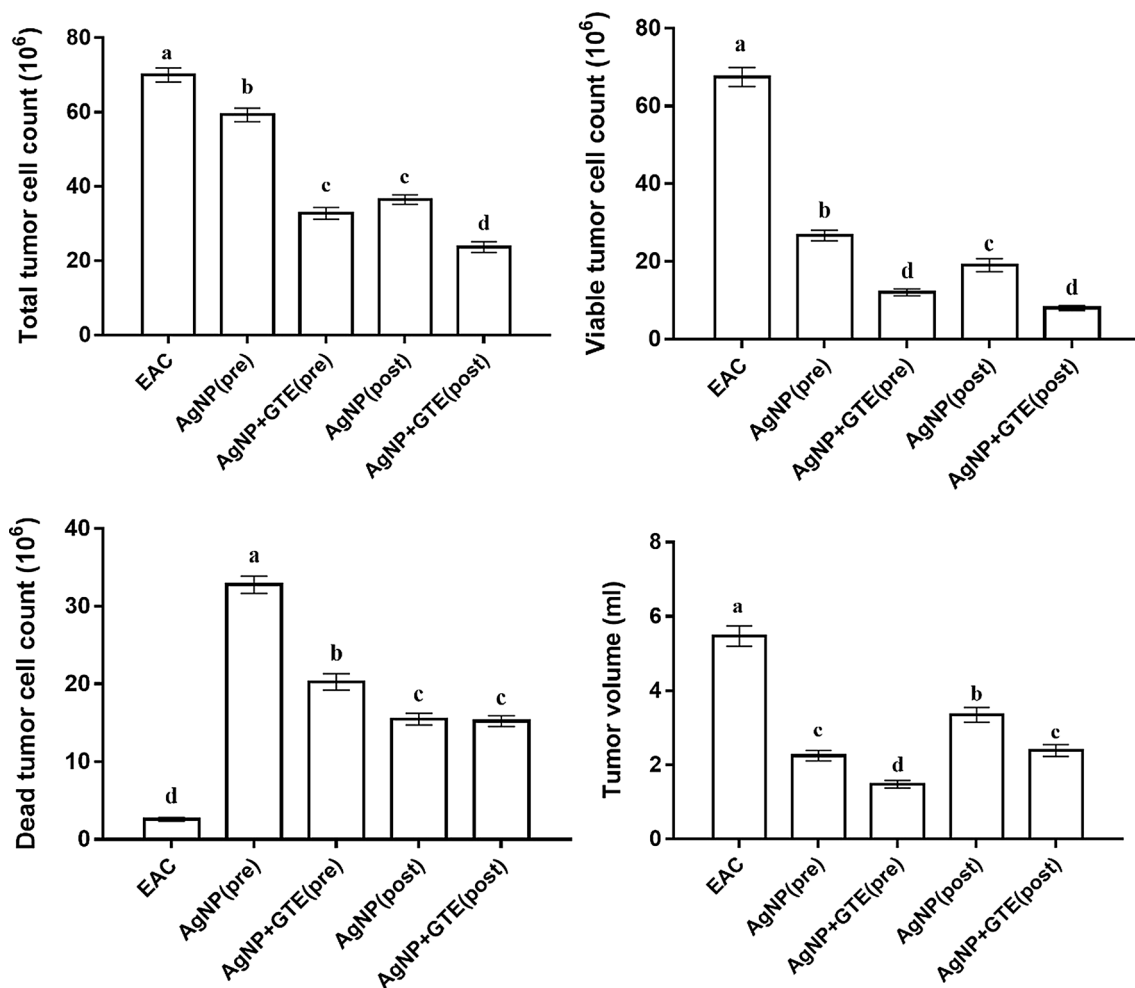


Fig. 2 Combined effect of AgNPs and GTE on total tumor cell count, viable and non-viable tumor cell count, and tumor volume. Values were expressed as mean \pm SEM. Means within columns carrying different superscript letters [a (highest)–d (lowest)] were significantly

different at $P \leq 0.05$. EAC (G2); AgNP(pre) (G3), AgNP+GTE (pre) (G4), AgNP(post) (G5), AgNP+GTE (post) (G6). *Pre* pre-treatment, *Post* post-treatment

central vein (arrowhead, Fig. 5a). In contrast, EAC group (G2) showed presence of a variable number of anaplastic metastatic cells (with enlarged, atypical, pleomorphic and hyperchromatic nuclei) distributed among hepatic cells (arrows) and around the dilated central vein (arrowhead, Fig. 5b). On the other hand, AgNPs pre-treated group (G3, Fig. 5c) showed a marked decrease in number of anaplastic metastatic cells, portal congestion (green arrowhead), mononuclear round cells aggregation (yellow arrowhead), and biliary proliferation (black arrowhead). Some hepatocytes appeared with large hyperchromatic nuclei and others were degenerated (arrows, Fig. 5c). AgNPs + GTE pre-treated group (G4) had apparently normal hepatic parenchyma with preserved cord arrangement and normal stroma (arrow, Fig. 5d). However, mice post-treated with AgNPs (G5) had congested portal vein (black arrowhead), interstitial aggregation of pro-inflammatory mononuclear

cells (yellow arrowhead), and hemosiderosis in some macrophages (arrows, Fig. 5e). Animals post-treated with AgNPs + GTE (G6) showed hepatocellular proliferative changes with moderate atypia (arrow), pleomorphism (black arrowhead) and hyperchromia (yellow arrowhead, Fig. 5f).

Effect of AgNPs and GTE on liver ultrastructure

Analysis of TEM images from the control group (G1) showed presence of normal hepatocytes (Fig. 6a). The hepatocyte had normal nucleus surrounded by intact nuclear membrane (NM, yellow arrow) and its nucleoplasm contained clear nucleolus (white arrow) with distinct eu- and heterochromatins. The cell organelles also appeared normal with a large number of normal spheroid mitochondria (MITO, red arrow) and rough endoplasmic reticulum (RER, blue arrow). However, hepatocytes of

Fig. 3 Combined effect of AgNPs and GTE on micronuclei distribution. **a, b** Representative photomicrographs from stained blood films showing micronuclei (arrows) within erythrocytes. Giemsa stain, X400 (**a**) and X1000 (**b**). **c** Histogram showing distribution of micronuclei in different groups. Values were expressed as mean \pm SEM. Means within columns carrying different superscript letters [a (highest)–c (lowest)] were significantly different at $P \leq 0.05$. Cnt (G1); EAC (G2); AgNP(pre) (G3), AgNP + GTE (pre) (G4), AgNP(post) (G5), AgNP + GTE (post) (G6). *Pre* pre-treatment, *Post* post-treatment

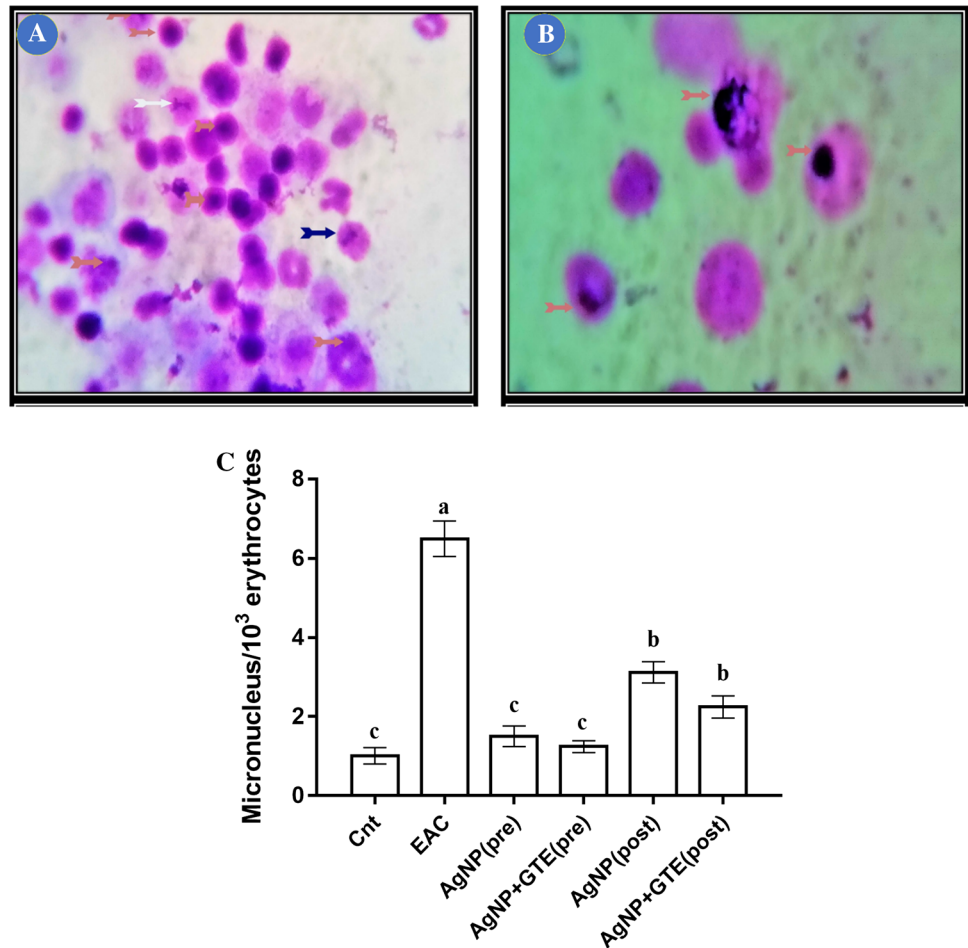


Table 1 Effects of AgNPs and GTE on chromosomal aberrations

Groups	Ring chromosome	Deletion	Centromeric attenuation	End-to-end association
Cnt (G1)	0.07 \pm 0.001 ^d	3.20 \pm 0.20 ^d	3.50 \pm 0.20 ^f	2.50 \pm 0.30 ^f
EAC (G2)	6.20 \pm 0.55 ^a	7.40 \pm 0.90 ^a	9.96 \pm 0.55 ^a	10.22 \pm 0.60 ^a
AgNP (pre) (G3)	4.20 \pm 0.35 ^{bc}	5.21 \pm 0.37 ^b	7.41 \pm 0.42 ^b	6.22 \pm 0.32 ^d
AgNP + GTE (pre) (G4)	3.40 \pm 0.24 ^c	4.15 \pm 0.34 ^c	5.84 \pm 0.30 ^c	3.91 \pm 0.28 ^e
AgNP (post) (G5)	5.34 \pm 0.42 ^b	6.21 \pm 0.42 ^b	8.06 \pm 0.31 ^b	8.84 \pm 0.43 ^b
AgNP + GTE (post) (G6)	3.55 \pm 0.34 ^c	5.08 \pm 0.39 ^c	6.28 \pm 0.34 ^c	7.31 \pm 0.38 ^c

Data were expressed as mean \pm SEM

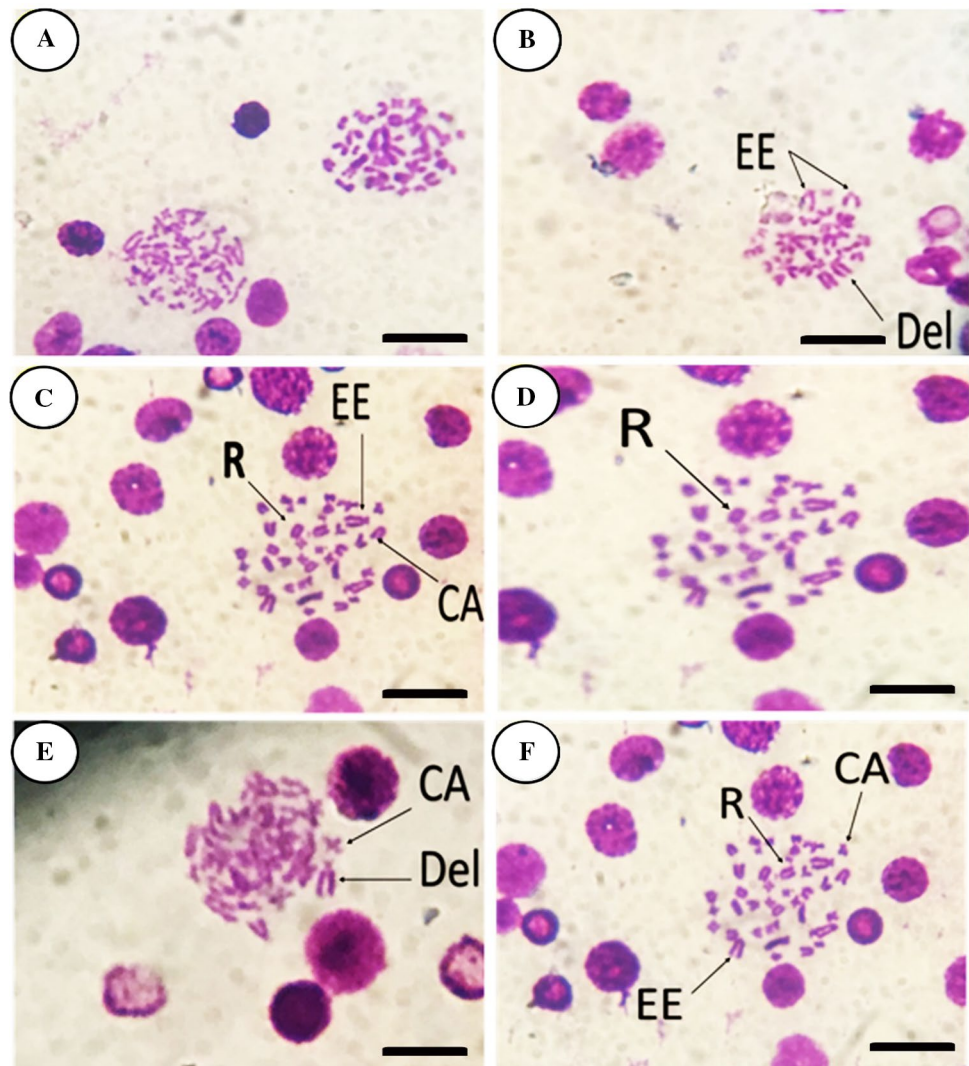
Pre pre-treatment, *Post* post-treatment

Values in the same column carrying different superscript letters [a (highest)–f (lowest)] were significantly different at $P \leq 0.05$

EAC mice (G2) exhibited some cytopathological alterations (Fig. 6b). The nucleus had indented nuclear membrane with small irregular nucleoli and both condensed and dispersed chromatin. The cytoplasm contained scanty mitochondria, but with abundant deformed rough and smooth endoplasmic reticulum (RER, SER), glycogen granules (blue star, GR), and numerous electron-dense bodies (EDB, Fig. 6b). Animals pre-treated with AgNPs (G3) showed notable cytopathological changes (Fig. 6c).

The cytoplasm contained numerous membranous enveloped vacuoles present inside phagolysosomes (blue circle, red arrowhead, and blue arrow) and was accompanied by a group of activated macrophages (white arrow) and electron-dense endosomes (orange arrows). The bile ductules (BD) were enwrapped by thick basal lamellar membrane (red and black arrows) and lined by short cuboidal epithelial cells (E.C, green arrow) with luminal side microvillous projections (M. villi, Fig. 6c). Hepatocytes

Fig. 4 Photomicrographs of metaphase spread from bone marrow cells of mice showing effect of AgNPs and GTE on chromosomal distribution. **a** Cnt (G1); **b** EAC (G2); **c** AgNP pre-treatment (G3); **d** AgNP+GTE pre-treatment (G4); **e** AgNP post-treatment (G5); and **f** AgNP+GTE post-treatment (G6). Giemsa stain, scale bar=100 μ m. CA centromeric attenuation, EE end-to-end association, Del deletion, R ring chromosome



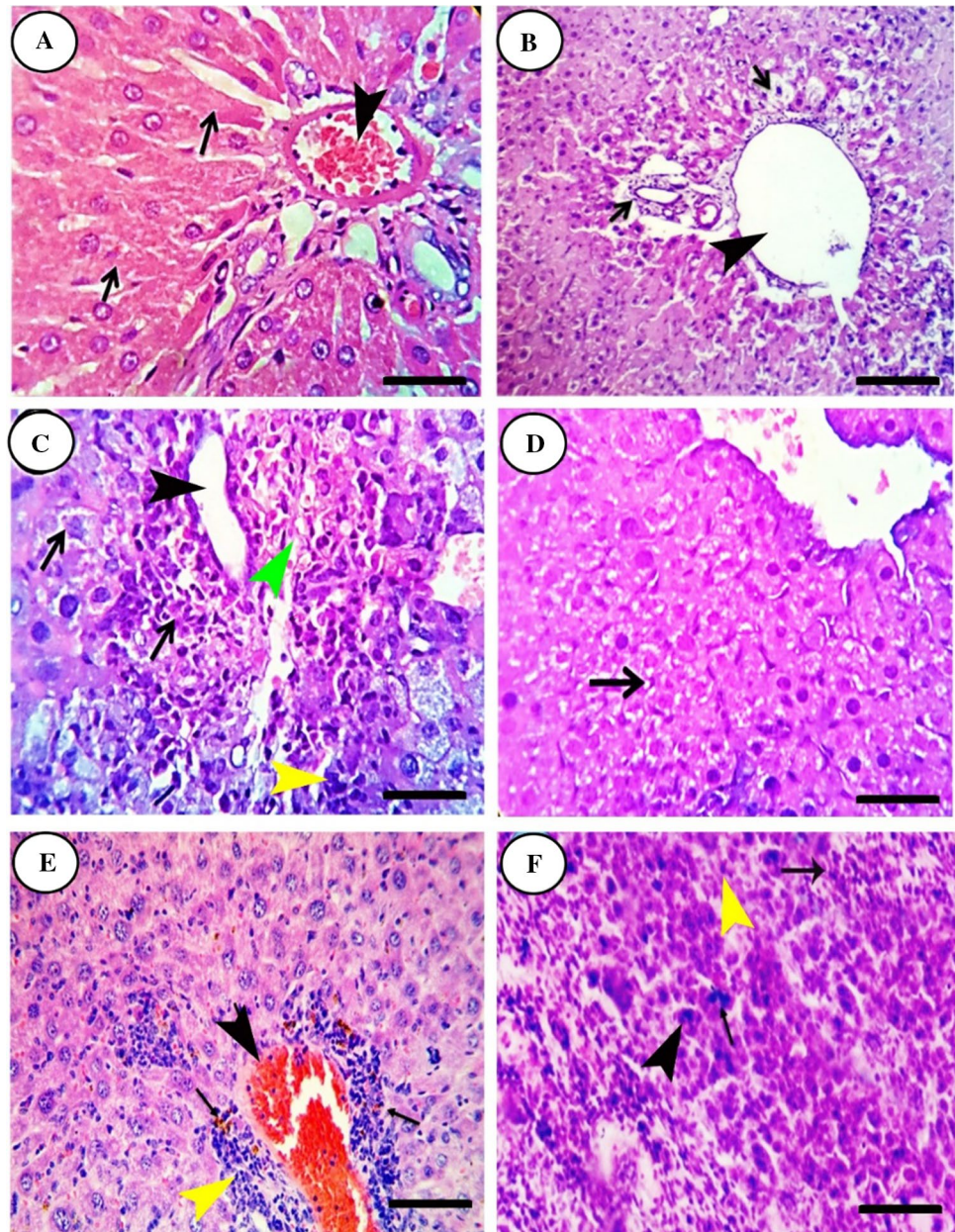
of the combined pre-treated group (G4) had less severe cytopathological changes (Fig. 6d). The hepatocytes contained phagolysosomes (blue circle) encompassing numerous endosomes (orange arrow). The cytoplasm had numerous ribosomes (white arrows), electron-dense small spherical bodies (EDB), membrane-bound vacuoles (red arrow) of variable size, and mitochondria (Fig. 6d). Hepatocytes of EAC mice post-treated with AgNPs showed active nuclear division (binucleation, blue arrow) and their cytoplasm contained numerous elongated electron-dense structures (green arrow), rounded ovo-spheroid bodies surrounded by bright halos (could be AgNPs, orange arrows), and cytoplasmic vacuoles of variable size (red arrow, Fig. 6e). Hepatocytes of combined post-treated animals (G6) had many mitochondria, rough endoplasmic reticulum (RER), and rounded ovo-spheroid bodies surrounded by bright halos (could be AgNPs, orange arrows,

Fig. 6f). Additionally, intercellular digitating membrane (blue arrow), desmosomes (red arrow) and bile canalicular microtubules (green arrow, Fig. 6f) were also seen.

Effect of GTE and AgNPs on MDA level and antioxidant enzyme activities

Untreated EAC mice and those treated with AgNPs alone showed significant increase in serum level of the lipid peroxidation biomarker MDA and significant decrease in activities of the antioxidant enzymes (SOD, GPx, and CAT) in serum as compared to the control mice (Table 2). These altered biochemical parameters were restored following either pre- or post-treatment with GTE and AgNPs, with best effect for pre-treated group, but their levels remained lower than that of the control group.

Fig. 5 Effect of AgNPs and GTE on liver histology as revealed by light microscope. **a** Liver of the control group (G1) showed normal hepatic cords (arrows) radiating from the central vein (arrowhead). **b** Liver of the EAC group (G2) showed anaplastic metastatic cells (arrows) and dilated central vein (arrowhead). **c** Liver of the AgNP pre-treatment group (G3) showed portal congestion (green arrowhead), mononuclear round cells aggregation (yellow arrowhead), biliary proliferation (black arrowhead), and some hepatocytes appeared with large hyperchromatic nuclei and others were degenerated (arrows). **d** Liver of the AgNP + GTE pre-treatment group (G4) showed normal hepatocytes (arrows). **e** Liver of the AgNP post-treatment group (G5) showed congested portal vein (black arrowhead), aggregated pro-inflammatory mononuclear cells (yellow arrowhead), and hemosiderosis (arrows). **f** Liver of the AgNP + GTE post-treatment group (G6) showed proliferation with moderate atypia (arrow), pleomorphism (black arrowhead) and hyperchromia (yellow arrowhead). H&E, scale bar = 50 μm (a, c, d, f) and 20 μm (b, e)



Discussion

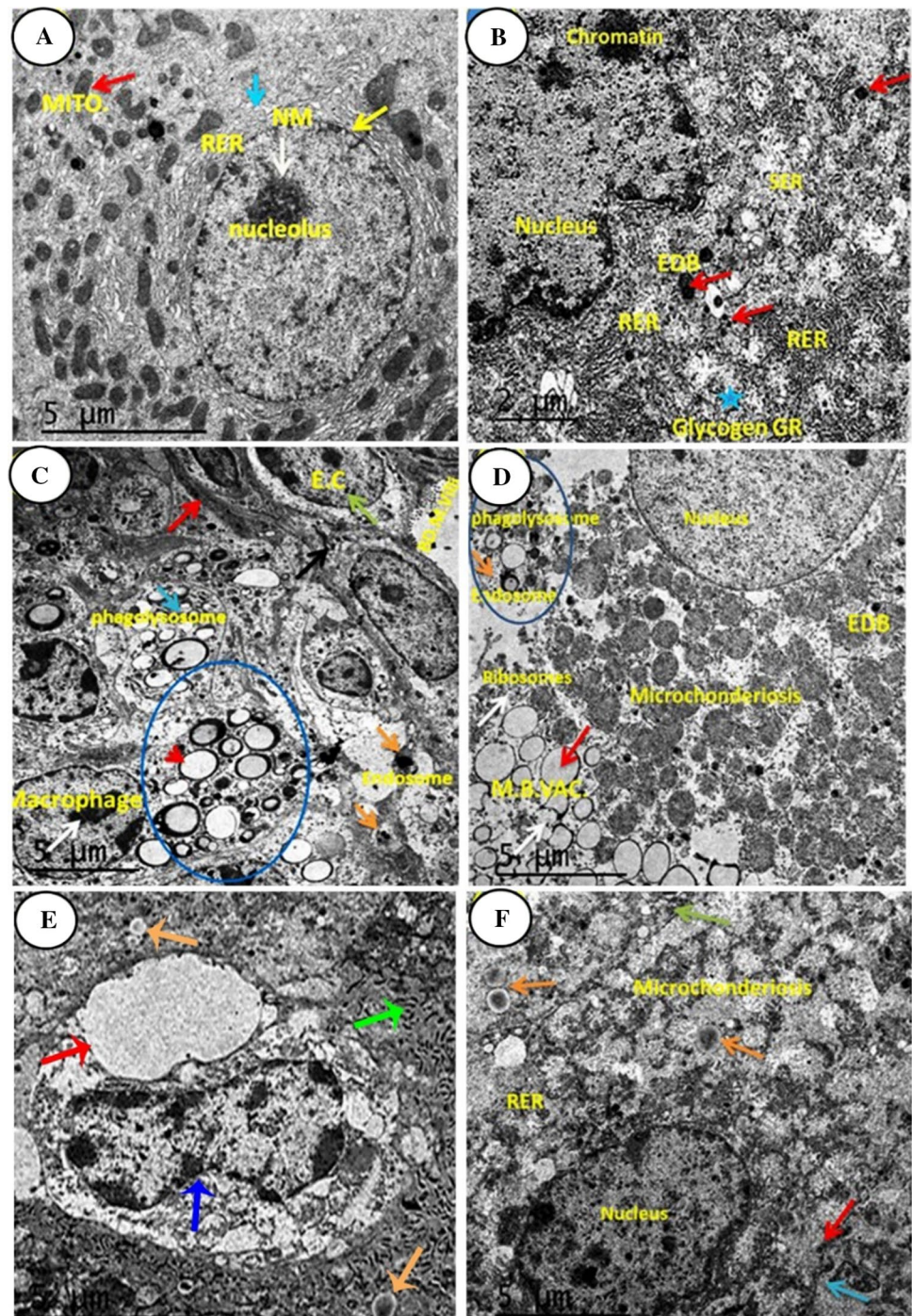
Previous studies reported potent anti-cancer effects for AgNPs (Devaraj et al. 2013; Gurunathan et al. 2015; Jeyaraj et al. 2013; Lin et al. 2014) with fewer side effects than chemotherapeutic agents. However, AgNPs, similar to the majority of other NPs, can adversely affect normal cells (Ahamed et al. 2008; Cho et al. 2018). To the best of our knowledge, this may be the first study to report that GTE can not only ameliorate AgNPs-induced adverse effects but also improve their anti-cancer effect against EAC in mice.

In the present study, we found that pre- and post-treatment with AgNPs and GTE significantly decreased the tumor volume (ascitic fluid), and the count of total and viable tumor

cells and significantly increased dead EAC cell count. This anti-cancer effect was previously reported, but for each compound alone in models other than EAC. AgNPs induced apoptosis-dependent oxidative stress in breast, ovarian, lung, and cervical cancer cells (Devaraj et al. 2013; Gurunathan et al. 2015; Jeyaraj et al. 2013; Kanipandian et al. 2019; Lin et al. 2014). Green tea and its active components also induced apoptosis in most cancers (Bettuzzi et al. 2006), but via a different mechanism of action which has not been fully elucidated yet (Miyata et al. 2018).

After confirming that GTE synergistically potentiates the anti-cancer effect of AgNPs against EAC cells, we evaluated whether GTE can ameliorate the geno-, cyto- and histotoxic effects of AgNPs. To check genotoxic effects, we applied

Fig. 6 Effect of AgNPs and GTE on liver ultrastructure as detected by transmission electron microscope. **a** Liver of the control group (G1), nuclear membrane (NM, yellow arrow), nucleolus (white arrow), mitochondria (MITO, red arrow), rough endoplasmic reticulum (RER, blue arrow). **b** Liver of the EAC group (G2), smooth endoplasmic reticulum (RER, SER), glycogen granules (blue star, GR), electron-dense bodies (EDB) (red arrow). **c** Liver of the AgNP pre-treatment group (G3), membranous enveloped vacuoles (blue circle, red arrowhead, and blue arrow), macrophages (white arrow), electron-dense endosomes (orange arrows), bile ductules (BD) enwrapped by thick basal lamellar membrane (red and black arrows) and lined by short cuboidal epithelial cells (E.C, green arrow) with luminal side microvillous projections (*M. villi*). **d** Liver of the AgNP + GTE pre-treatment group (G4), phagolysosomes (blue circle), endosomes (orange arrow), ribosomes (white arrows), electron-dense small spherical bodies (EDB), membrane-bound vacuoles (red arrow). **e** Liver of the AgNP post-treatment group (G5), nuclear division (blue arrow), electron-dense structures (green arrow), rounded ovo-spheroid bodies (orange arrows), cytoplasmic vacuoles (red arrow). **f** Liver of the AgNP + GTE post-treatment group (G6), rough endoplasmic reticulum (RER), rounded ovo-spheroid bodies (orange arrows), intercellular digitating membrane (blue arrow), desmosomes (red arrow) and bile canicular microtubules (green arrow). Scales bars = 5 μ m



micronucleus and chromosomal aberrations assays and the obtained results confirmed our hypothesis that pre- and post-treatment with GTE and AgNPs relived the genotoxicity induced using AgNPs alone. The cyto- and histotoxic effects of AgNPs were evaluated by detection of cytological and histological changes in liver tissues using TEM and light microscope, respectively. Expectedly, treatment with AgNPs (with size range of 10–50 nm) alone produced several degenerative histological alterations in the hepatic

tissue including congested portal vein, infiltration of proinflammatory mononuclear cells (mainly leucocytes), biliary proliferation, hemosiderosis in some macrophage cells, and vacuolation, suggesting that AgNPs could induce hepatotoxicity when administered at therapeutic dose. Similar hepatotoxic effect was reported in mice (Cho et al. 2018) and rats (Sarhan and Hussein, 2014) intraperitoneally injected with small AgNPs (10 nm/mice and 20–60 nm/rats). Moreover, very small AgNPs (4 nm) were reported to induce higher

Table 2 Combined effect of AgNPs and GTE on malondialdehyde (MDA) levels and activity of superoxide dismutase (SOD), glutathione peroxidase (GPX) and catalase (CAT) enzymes in serum

Groups	MDA (nmol/ml)	SOD (U/L)	GPx (U/L)	CAT (U/L)
Cnt (G1)	12.43 ± 0.54 ^f	26.65 ± 0.90 ^a	70.27 ± 3.71 ^a	58.04 ± 2.18 ^a
EAC (G2)	37.01 ± 1.72 ^a	6.65 ± 0.36 ^f	22.27 ± 1.31 ^f	21.55 ± 1.07 ^f
AgNP (pre) (G3)	25.43 ± 0.80 ^c	10.85 ± 0.51 ^d	38.62 ± 1.26 ^d	36.47 ± 1.12 ^d
AgNP + GTE (pre) (G4)	16.37 ± 0.45 ^e	22.30 ± 0.94 ^b	58.52 ± 2.24 ^b	48.92 ± 1.75 ^b
AgNP (post) (G5)	29.11 ± 0.93 ^b	8.52 ± 0.46 ^e	31.62 ± 1.01 ^e	27.32 ± 1.07 ^e
AgNP + GTE (post) (G6)	21.28 ± 0.50 ^d	18.85 ± 0.70 ^c	49.23 ± 2.05 ^c	42.11 ± 1.15 ^c

Data were expressed as mean ± SEM

Pre pre-treatment, *Post* post-treatment

Values in the same column carrying different superscript letters [a (highest)–f (lowest)] were significantly different at $P \leq 0.05$

levels of free radicals, ROS, and IL8 from macrophages than larger AgNPs (70 nm) (Park et al. 2011). However, mice treated with larger AgNPs (60 nm and 100 nm) showed no histopathological changes in liver and other body organs (kidney, brain, lung, testis, spleen) (Cho et al. 2018; Kanipandian et al. 2019). Thus, it is likely that the particle size is the main determinant for AgNPs toxicity. Other factors may also play an important role in this toxicity including concentration, exposure time and route of administration for AgNPs (Genter et al. 2012). Small AgNPs have higher dissolution enabling them to easily penetrate the cell membrane and accumulate inside the cells at higher concentrations and quicker than the large AgNPs (Ji et al. 2007). Liver has been considered as one of the main target organs for AgNPs accumulation particularly within hepatic Kupffer cells which appeared as electron-dense materials under TEM (Sarhan and Hussein, 2014). Again, pre- and post-treatment by GTE and AgNPs relieved most of these histological changes thereby confirming the ability of GTE to ameliorate AgNPs-induced hepatotoxicity.

So, the question now is how AgNPs induced these geno-, cyto- and histotoxicities and how GTE can relieve them. It is well known that AgNPs, similar to most of NPs, exert their anti-bacterial, anti-fungal, and anti-cancer effects through induction of oxidative stress (Anandalakshmi et al. 2016; Devaraj et al. 2013; Gurunathan et al. 2015; Lee et al. 2019; Lin et al. 2014). It is likely that this effect is not specific to cancer cells and microorganisms and AgNPs may also target normal cells by the same mechanism. Indeed, apoptosis of fibroblast, muscle, and colon cells triggered by AgNPs treatment is mediated by oxidative stress (Foldbjerg et al. 2009). Additionally, AgNPs administration led to increased levels of MDA and reduced antioxidant marker levels and activities (GSH, SOD, CAT and GPx) in rat testis (Ansar et al. 2017). Moreover, hepatic oxidative damage was also induced by intraperitoneal injection of AgNPs in rats (Parang and Moghadamnia, 2018; Sarhan and Hussein, 2014). Similarly, we and Ebabe Elle et al. (2013) also found induction of higher oxidative stress status [as indicated by

marked elevation of MDA level and reduction in activities of antioxidant enzymes (SOD, GPx, and CAT)] in EAC mice serum and rats' livers, respectively, following treatment with AgNPs. It is therefore likely that AgNPs generated free radicals which attacked hepatocytes causing geno-, cyto-, and histotoxicities. Increased ROS production inside the cells induce damage of different cell components and molecules (protein, lipid, and DNA) leading to oxidative damage of plasma membrane, mitochondria, and nucleus which cause cell death (Abdelhady et al. 2017; Abu Gazia and El-Magd, 2018a, b; El-Magd et al. 2016; Zhao et al. 2004). AgNPs can also induce genotoxicity through interaction with thiol group of vital enzymes and phosphate groups of nucleic acid (Klueh et al. 2000). Unlike AgNPs, GTE and its phytochemicals are potent natural antioxidants. Indeed, pre- and post-treatment with GTE and AgNPs restored MDA, SOD, GPx and CAT to levels comparable to normal. This decreased the extent of oxidative damage and prevented geno-, cyto-, and histotoxicities triggered by AgNPs and EAC cells. The antioxidant activity of GTE may be one of the most probable mechanisms that help to prevent AgNPs toxicities.

GTE and AgNPs pre-treatment showed better effects than post-treatment in term of increasing the anti-cancer effect on EAC cells and decreasing geno-, cyto- and histotoxicities indicating the significance of GTE and AgNPs in prevention of EAC. Although the present study indicates for the first time the importance of combination therapy of GTE and AgNPs in EAC, it did not determine the actual molecular (at genes and proteins levels) mechanism by which GTE ameliorates AgNPs toxicity and potentiates their anti-cancer effect. So, further molecular investigations are required to fill in this scientific gap.

In summary, to the best of our knowledge, this may be the first study to report that GTE, as a potent natural antioxidant, can not only ameliorate AgNPs-induced oxidative stress-based adverse effects (geno-, cyto-, and histotoxicities) but also improve their anti-cancer effect against EAC in mice. Therefore, GTE could be used as a neoadjuvant in the treatment of AgNPs-induced geno-, cyto-, and histotoxicity,

however, further clinical investigations are needed to confirm whether this combination is clinically relevant in human.

Author contributions AM and NH involved in design, data collection, writing, and revising the manuscript. ES, NH and MK involved in conception, design, literature review, writing the manuscript. ME involved in design, writing, revising the manuscript. NA participated in responding on reviewers' comments. Additionally, all authors have read and approved the final manuscript.

Funding This study did not receive any grant from any funding agency.

Compliance with ethical standards

Conflict of interest The authors declare no conflict of interest.

Ethical approval All experiments were conducted in accordance with US National Institutes of Health Guidelines for the Care and Use of Laboratory Animals and followed Helsinki Declaration of animal ethics. This study was approved by the Research Ethics Committee of Kafrelsheikh University.

References

- Abdel-Daim MM, Moustafa YM, Umezawa M, Ramana KV, Azzini E (2017) Applications of antioxidants in ameliorating drugs and xenobiotics toxicity: mechanistic approach. *Oxid Med Cell Long* 2017:2
- Abdelhady D, El-Abasy M, Abou-Asa S, Elbially Z, Shukry M, Hussein A, Saleh A, El-Magd M (2017) The ameliorative effect of *Aspergillus awamori* on aflatoxin B1-induced hepatic damage in rabbits. *World Mycotoxin J* 10:363–373
- Abu Gazia M, El-Magd MA (2018a) Ameliorative effect of cardamom aqueous extract on doxorubicin-induced cardiotoxicity in rats. *Cells Tissues Organs* 206:62–72
- Abu Gazia M, El-Magd MA (2018b) Effect of pristine and functionalized multiwalled carbon nanotubes on rat renal cortex. *Acta Histochem* 121(2):207–217
- Abu Khudir R, El-Magd MA, Salama AF, Tousson EM, El-Dsoki SM (2019) Curcumin attenuated oxidative stress and inflammation on hepatitis induced by fluvastatin in female albino rats. *Alex J Vet Sci* 62(1):102–115
- Ahamed M, Karns M, Goodson M, Rowe J, Hussain SM, Schlager JJ, Hong Y (2008) DNA damage response to different surface chemistry of silver nanoparticles in mammalian cells. *Toxicol Appl Pharmacol* 233:404–410
- Anandalakshmi K, Venugobal J, Ramasamy V (2016) Characterization of silver nanoparticles by green synthesis method using *Petalium murex* leaf extract and their antibacterial activity. *Appl Nanosci* 6:399–408
- Ansar S, Abudawood M, Hamed SS, Aleem MM (2017) Sodium selenite protects against silver nanoparticle-induced testicular toxicity and inflammation. *Biol Trace Elem Res* 175:161–168
- Badawy AA, El-Magd MA, AlSadrh SA (2018) Therapeutic effect of camel milk and its exosomes on MCF7 cells in vitro and in vivo. *Integr Cancer Ther* 7:1235–1246
- Badawy A, Hassanean H, Ibrahim AK, Habib ES, El-Magd MA, Ahmed SA (2019) Isolates from *Thymelaea hirsuta* inhibit progression of hepatocellular carcinoma in vitro and in vivo. *Nat Prod Res*. <https://doi.org/10.1080/14786419.2019.1643859>
- Bettuzzi S, Brausi M, Rizzi F, Castagnetti G, Peracchia G, Corti A (2006) Chemoprevention of human prostate cancer by oral administration of green tea catechins in volunteers with high-grade prostate intraepithelial neoplasia: a preliminary report from a one-year proof-of-principle study. *Cancer Res* 66:1234–1240
- Chacko SM, Thambi PT, Kuttan R, Nishigaki I (2010) Beneficial effects of green tea: a literature review. *Chin Med* 5:13
- Cho YM, Mizuta Y, Akagi JI, Toyoda T, Sone M, Ogawa K (2018) Size-dependent acute toxicity of silver nanoparticles in mice. *J Toxicol Pathol* 31:73–80
- Devaraj P, Kumari P, Aarti C, Renganathan A (2013) Synthesis and characterization of silver nanoparticles using cannonball leaves and their cytotoxic activity against MCF-7 cell line. *J Nanotechnol* 2013:5
- Ebabe Elle R, Gaillet S, Vide J, Romain C, Lauret C, Rugani N, Cristol JP, Rouanet JM (2013) Dietary exposure to silver nanoparticles in Sprague–Dawley rats: effects on oxidative stress and inflammation. *Food Chem Toxicol* 60:297–301
- El-Bayomi KM, Saleh AA, Awad A, El-Tarabany MS, El-Qalioubi HS, Afifi M, El-Komy S, Essawi WM, Almadaly EA, El-Magd MA (2018) Association of CYP19A1 gene polymorphisms with anoestrus in water buffaloes. *Reprod Fertil Dev* 30:487–497
- Elgazar AA, Selim NM, Abdel-Hamid NM, El-Magd MA, El Hefnawy HM (2018) Isolates from *Alpinia officinarum* hance attenuate LPS induced inflammation in HepG2: evidence from in silico and in vitro studies. *Phytother Res* 32:1273–1288
- Elkeiy M, Khamis A, El-Gamal M, Abo Gazia M, Zalut Z, El-Magd M (2018) Chitosan nanoparticles from *Artemia salina* inhibit progression of hepatocellular carcinoma in vitro and in vivo. *Environ Sci Pollut Res Int*. <https://doi.org/10.1007/s11356-018-3339-6>
- El-Magd MA, Kahilo KA, Nasr NE, Kamal T, Shukry M, Saleh AA (2016) A potential mechanism associated with lead-induced testicular toxicity in rats. *Andrologia* 49:e12750
- El-Magd MA, Khamis A, Nasr Eldeen SK, Ibrahim WM, Salama AF (2017) Trehalose enhances the antitumor potential of methotrexate against mice bearing Ehrlich ascites carcinoma. *Biomed Pharmacother* 92:870–878
- El-Magd MA, Mohamed Y, El-Shetry ES, Elsayed SA, Abo Gazia M, Abdel-Aleem GA, Shafik NM, Abdo WS, El-Desouki NI, Basyony MA (2019) Melatonin maximizes the therapeutic potential of non-preconditioned MSCs in a DEN-induced rat model of HCC. *Biomed Pharmacother* 114:108732
- Fenech M, Chang WP, Kirsch-Volders M, Holland N, Bonassi S, Zeiger E (2003) HUMN project: detailed description of the scoring criteria for the cytokinesis-block micronucleus assay using isolated human lymphocyte cultures. *Mutat Res* 534:65–75
- Foldbjerg R, Olesen P, Hougard M, Dang DA, Hoffmann HJ, Autrup H (2009) PVP-coated silver nanoparticles and silver ions induce reactive oxygen species, apoptosis and necrosis in THP-1 monocytes. *Toxicol Lett* 190:156–162
- Fujiki H, Suganuma M, Imai K, Nakachi K (2002) Green tea: cancer preventive beverage and/or drug. *Cancer Lett* 188:9–13
- Genter MB, Newman NC, Shertzer HG, Ali SF, Bolon B (2012) Distribution and systemic effects of intranasally administered 25 nm silver nanoparticles in adult mice. *Toxicol Pathol* 40:1004–1013
- Gottesman MM, Fojo T, Bates SE (2002) Multidrug resistance in cancer: role of ATP-dependent transporters. *Nat Rev Cancer* 2:48–58
- Gurunathan S, Han JW, Park JH, Kim E, Choi YJ, Kwon DN, Kim JH (2015) Reduced graphene oxide-silver nanoparticle nanocomposite: a potential anticancer nanotherapy. *Int J Nanomed* 10:6257–6276
- Jeyaraj M, Sathishkumar G, Sivanandhan G, MubarakAli D, Rajesh M, Arun R, Kapildev G, Manickavasagam M, Thajuddin N, Premkumar K, Ganapathi A (2013) Biogenic silver nanoparticles for

- cancer treatment: an experimental report. *Colloids and surfaces. B, Biointerfaces* 106:86–92
- Ji JH, Jung JH, Kim SS, Yoon JU, Park JD, Choi BS, Chung YH, Kwon IH, Jeong J, Han BS, Shin JH, Sung JH, Song KS, Yu IJ (2007) Twenty-eight-day inhalation toxicity study of silver nanoparticles in Sprague-Dawley rats. *Inhal Toxicol* 19:857–871
- Jia J, Li F, Zhou H, Bai Y, Liu S, Jiang Y, Jiang G, Yan B (2017) Oral exposure to silver nanoparticles or silver ions may aggravate fatty liver disease in overweight mice. *Environ Sci Technol* 51:9334–9343
- Kanipandian N, Li D, Kannan S (2019) Induction of intrinsic apoptotic signaling pathway in A549 lung cancer cells using silver nanoparticles from *Gossypium hirsutum* and evaluation of in vivo toxicity. *Biotechnol Rep (Amsterdam, Netherlands)* 23:e00339
- Khamis AAA, Ali EMM, El-Moneim MAA, Abd-Alhaseeb MM, El-Magd MA, Salim EI (2018) Hesperidin, piperine and bee venom synergistically potentiate the anticancer effect of tamoxifen against breast cancer cells. *Biomed Pharmacother* 105:1335–1343
- Klueh U, Wagner V, Kelly S, Johnson A, Bryers JD (2000) Efficacy of silver-coated fabric to prevent bacterial colonization and subsequent device-based biofilm formation. *J Biomed Mater Res* 53:621–631
- Lee B, Lee MJ, Yun SJ, Kim K, Choi IH, Park S (2019) Silver nanoparticles induce reactive oxygen species-mediated cell cycle delay and synergistic cytotoxicity with 3-bromopyruvate in *Candida albicans*, but not in *Saccharomyces cerevisiae*. *Int J Nanomed* 14:4801–4816
- Lin J, Huang Z, Wu H, Zhou W, Jin P, Wei P, Zhang Y, Zheng F, Zhang J, Xu J, Hu Y, Wang Y, Li Y, Gu N, Wen L (2014) Inhibition of autophagy enhances the anticancer activity of silver nanoparticles. *Autophagy* 10:2006–2020
- Marimuthu S, Rahuman AA, Rajakumar G, Santhoshkumar T, Kirthi AV, Jayaseelan C, Bagavan A, Zahir AA, Elango G, Kamaraj C (2011) Evaluation of green synthesized silver nanoparticles against parasites. *Parasitol Res* 108:1541–1549
- Miyata Y, Matsuo T, Araki K, Nakamura Y, Sagara Y, Ohba K, Sakai H (2018) Anticancer effects of green tea and the underlying molecular mechanisms in bladder cancer. *Medicines (Basel)* 5(3):87–98
- Mohamed Y, Basyony MA, El-Desouki NI, Abdo WS, El-Magd MA (2019) The potential therapeutic effect for melatonin and mesenchymal stem cells on hepatocellular carcinoma. *BioMedicine* 9:23–29
- Pacchierotti F, Stocchi V (2013) Analysis of chromosome aberrations in somatic and germ cells of the mouse. *Methods Mol Biol (Clifton, NJ)* 1044:147–163
- Parang Z, Moghadamnia D (2018) Effects of silver nanoparticles on the functional tests of liver and its histological changes in adult male rats. *Nanomed Res J* 3:146–153
- Park J, Lim DH, Lim HJ, Kwon T, Choi JS, Jeong S, Choi IH, Cheon J (2011) Size dependent macrophage responses and toxicological effects of Ag nanoparticles. *Chem Commun (Camb)* 47:4382–4384
- Safer AM, Afzal M, Nomani A, Sosamma O, Mousa SA (2012) Curative propensity of green tea extract towards hepatic fibrosis induced by CCl₄: a histopathological study. *Exp Ther Med* 3:781–786
- Sarhan OM, Hussein RM (2014) Effects of intraperitoneally injected silver nanoparticles on histological structures and blood parameters in the albino rat. *Int J Nanomed* 9:1505–1517
- Zhao K, Zhao GM, Wu D, Soong Y, Birk AV, Schiller PW, Szeto HH (2004) Cell-permeable peptide antioxidants targeted to inner mitochondrial membrane inhibit mitochondrial swelling, oxidative cell death, and reperfusion injury. *J Biol Chem* 279:34682–34690

Publisher's Note Springer Nature remains neutral with regard to jurisdictional claims in published maps and institutional affiliations.